Postharvest Biology and Technology 78 (2013) 67–75

Contents lists available at SciVerse ScienceDirect

Postharvest Biology and Technology

journal homepage: www.elsevier.com/locate/postharvbio

Profiling shifts in protein complement in tomato fruit induced by atmospheric ozone-enrichment and/or wound-inoculation with *Botrytis cinerea*

Nikos Tzortzakis[2], Tahar Taybi[1], Edna Antony[1], Ian Singleton[1], Anne Borland[1], Jeremy Barnes[*,1]

Environmental and Molecular Plant Physiology, Newcastle Institute for Research on Sustainability, School of Biology, Newcastle University, Newcastle upon Tyne NE1 7RU, UK

ARTICLE INFO

Article history:
Received 17 October 2012
Received in revised form
16 December 2012
Accepted 18 December 2012

Keywords:
Tomato fruit
Ozone
Botrytis cinerea
Modified atmosphere storage
Proteomics

ABSTRACT

To unravel the mechanism by which low level atmospheric ozone-enrichment (0.05 μmol mol^{-1}) increases the shelf-life of tomato fruit (*Lycopersicon esculentum* Mill.) by suppressing the growth of pathogens (*Botrytis cinerea*), protein yield and composition were examined during and following exposure to the gas at 13 °C/95% RH. Ozone-enrichment caused marked changes in protein yield and composition in control tomato fruit and suppressed shifts in the proteome induced by wounding/fungal attack. Wound/fungal-inoculation with *B. cinerea* resulted in a 7% increase in protein yield, and the down-regulation of at least 32 proteins. A number of proteins affected under ozone and wound/fungal-inoculation treatments are involved in the control of cellular oxidative status. Proteins that may be enhanced under oxidative stress were induced during ozone exposure (e.g. thioredoxin peroxidase-TPX), but suppressed following transfer to 'clean air' (e.g. ascorbate peroxidase-APX1). Constitutively-expressed proteins tended to increase reversibly under ozone-treatment, however proteins involved in ripening such as an enzyme related to ethylene biosynthesis (1-aminocyclopropane-1-carboxylate oxidase-ACO) were markedly reduced in ozone-treated tomato fruit but increased in wound-inoculated fruit. Levels of proteins involved in carbohydrate metabolism, pentose phosphate pathway, terpenoid and flavonoid biosynthesis differentiated among the treatments. The presented dataset makes a central contribution to a comprehensive analysis of the manner in which tomato fruit react to ozone-enrichment and/or pathogen infection during storage/transit.

1. Introduction

Much postharvest research has focused on improvement in the handling and preservation of fresh produce. There are growing health and environmental concerns over current treatment practices due to concerns over potentially carcinogenic residues resulting from agrochemical inputs to preserve fresh produce and extend its shelf-life (Spotts and Peters, 1980). Alternative solutions are currently sought to minimise pre- and postharvest dependence on agrochemical inputs with considerable interest currently being expressed in alternative, safer, 'environmental-friendly', sanitising agents, including ozone (Rice, 2002).

Ozone is an efficient anti-bacterial and anti-viral agent that has been used safely in the treatment of drinking water since the 1800s. Several reports have cited ozone as a viable alternative to traditional sanitisers (e.g. chlorine and bromide-based products) for the postharvest treatment of a variety of fresh fruit and vegetables (Xu, 1999; Tzortzakis et al., 2007). In 1997, an expert panel in conjunction with the US Food and Drug Administration (FDA), gave ozone 'Generally Recognised As Safe' (GRAS) status for use in direct food contact applications (Graham et al., 1997) and the gas received official approval for use as a direct contact Food Additive in 2003. Legislation allowing the deployment of ozone for various applications in the food sector has driven worldwide interest in hastening the potential afforded by the gas.

Although the efficacy of ozone as sanitiser of fresh fruit and vegetables is well proven, the mechanism by which the gas achieves this effect remains poorly understood. Previous work has shown that ozone affects severely sporulation of *Botrytis cinerea* reducing the propagation of the disease and its impact on spoilage of fresh produce (Tzortzakis et al., 2007). Moreover ozone was shown to induce dramatic changes in the physiology of the fruit in tomato in terms of fruit response to the pathogen as suggested

* Corresponding author at: Environmental and Molecular Plant Physiology, Newcastle Institute for Research on Sustainability, School of Biology, Devonshire Building, Newcastle University, Newcastle Upon Tyne NE1 7RU, UK. Tel.: +44 191 222 3432.
E-mail address: j.d.barnes@ncl.ac.uk (J. Barnes).
[1] Present address: Environmental and Molecular Plant Physiology, Newcastle Institute for Research on Sustainability, School of Biology, Newcastle University, Newcastle Upon Tyne NE1 7RU, UK.
[2] Present address: Department of Agricultural Sciences, Biotechnology and Food Science, Faculty of Geotechnical Sciences and Environmental Management, Cyprus University of Technology, Limassol, Cyprus.

0925-5214/$ – see front matter © 2012 Elsevier B.V. All rights reserved.
http://dx.doi.org/10.1016/j.postharvbio.2012.12.005

by the strong down-regulation of pathogen-resistant genes (*Chit* and *Gluc* and *Pdf1.2*) and signalling genes (*Aco1* and *Aso1* and *Hpl1*) (Tzortzakis et al., 2011). Sarig et al. (1996) showed that moderate ozone-enrichment (0.2 μmol mol^{-1}) resulted in enhanced levels of antifungal compounds (e.g. resveratrol and pterostilbene) in table grapes, and this effect was associated with pronounced benefits in terms of 'shelf-life' when fruit were subsequently removed from the ozone-enriched environment in which they have been stored. Minas et al. (2010) showed that pre-inoculation exposure to ozone may stimulate host resistance and accumulation of phenolic compounds in kiwifruit.

Work on the impacts of ozone on foliage indicates that ozone may influence the responses of plant tissue to a variety of biotic and abiotic stresses, including diseases (Tonneijck and Leone, 1993). Thus, ozone appears to act by inducing a hypersensitive response (HR) in plant tissue mimicking the biochemical and molecular events induced by pathogens and other stress factors (Rao et al., 2000). Ozone has been shown to activate an oxidative burst in leaves, similar to plant pathogen attack, which results in the accumulation of reactive oxygen species (ROS) such as superoxide radicals (O_2^-) and hydrogen peroxide (H_2O_2) (Rao et al., 2000). Ozone-induced ROS are believed to activate distinct signalling pathways dependent on salicylic acid, jasmonic acid and ethylene and induce a wide array of defence reactions including HR-associated cell death plus the induction of PR-proteins and antimicrobial defences (Overmyer et al., 2000; Rao et al., 2000).

Proteomics approaches including high resolution two-dimensional electrophoresis (2DE), in-gel proteolytic digestion of protein spots and protein identification by mass spectrometry (i.e. peptide mass fingerprinting (PMF)), are routinely used to identify shifts in the proteome associated with plant development, the reaction of plant tissues to a variety of biotic and abiotic stresses and quality-related aspects of fruit, salads and vegetables. Most studies have focused principally on rice (*Oryza sativa* L.) (Gammulla et al., 2011; Liu et al., 2011), barley (*Hordeum vulgare* L.) (Finnie et al., 2011), wheat (*Triticum aestivum* L.) (Bykova et al., 2011), as well as the model plant *Arabidopsis thaliana* L. (Huang et al., 2011) because of the available sequence information to facilitate protein identification (Rabilloud, 2000; Corpillo et al., 2004). In tomato (*Lycopersicon esculentum* Mill.), proteomics approaches were applied to investigate different aspects including responses to pathogens (Rep et al., 2002; Dahal et al., 2009), viruses (Corpillo et al., 2004; Casado-Vela et al., 2006), abiotic-stresses (Chen et al., 2009; Hahn et al., 2011) as well as metabolism and development (Barsan et al., 2010; Schilmiller et al., 2010; Catalá et al., 2011). Previous proteome reports on tomato fruit subjected to heat stress or blossom-end rot showed induced antioxidant processes (ascorbate–glutathione cycle) and the pentose phosphate pathway suggesting that these two biochemical pathways, might be associated with increased scavenging of reactive oxygen species in tomato fruit (Iwahashi and Hosoda, 2000; Saravanan and Rose, 2004; Casado-Vela et al., 2005).

The rapid growth in tomato expressed sequence tag (EST) data resulted in the recent tomato genome sequencing (May 2012). Up to now, combined information from related species (including potato, *Solanum tuberosum* L.), tobacco (*Nicotiana tabacum* L.), watermelon (*Citrullus lanatus* L.), and *A. thaliana*, has constituted a useful source of information for protein identification in tomato fruit (Saravanan and Rose, 2004).

In the present study, the impacts of atmospheric ozone-enrichment and/or *B. cinerea* infection on the proteome of tomato fruit were investigated within the *p*I range 3–10 and/or 4–7. The presented dataset represent the first report of protein shifts induced under ozone and/or pathogen infection in tomato fruit and provides key information on the putative mechanism behind the ozone-induced fruit-resistance to pathogens.

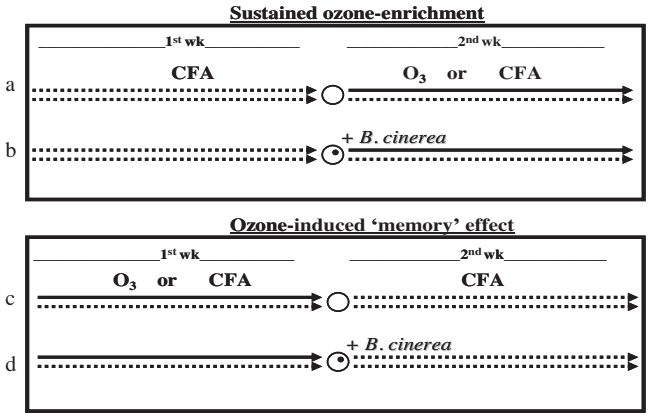

Fig. 1. Tomato fruit were maintained in CFA (·····▶) for 1 week prior to transferring batches of fruit to 'clean air' (CFA) or ozone (0.05 μmol mol^{-1}) (→) for 1 week (a) or post-inoculation as wound-inoculated with *B. cinerea* (b). A third batch of fruit was exposed to ozone (0.05 μmol mol^{-1}) for 1 week then transferred to controlled environment chambers ventilated with CFA for 1 more week (c) or wound-inoculated with *B. cinerea* and stored for 1 week (d) where the fruit were maintained at 13 °C, 95% RH in the dark.

2. Materials and methods

2.1. Plant material and experimental design

Mature, organically-grown tomato fruit (*L. esculentum* Mill. cv. Carousel) were selected for uniformity in size (47–57 mm) and appearance, and the absence of physical defects. To determine the influence of ozone exposure on disease development, tomato fruit were maintained in charcoal-filtered 'clean air' (CFA) for 1 week prior to transferring batches of fruit to CFA or ozone (0.05 μmol mol^{-1}) for 1 more week (Fig. 1a). In a second set of fruit (Fig. 1b), replicate batches of fruit (exposed as in Fig. 1a) were wound-inoculated with *B. cinerea* prior to ozone-enrichment with a mycelial plug (2.5 mm diameter) removed from the advancing margins of a 3-day-old culture of *B. cinerea*. To investigate 'memory effects', a third batch of fruit (Fig. 1c) was exposed to ozone (0.05 μmol mol^{-1}) for 1 week, then transferred to controlled environment chambers ventilated with CFA. A forth batch of fruit (Fig. 1d) was exposed to CFA or ozone (0.05 μmol mol^{-1}) for 1 week then wound-inoculated with *B. cinerea* prior to transfer to controlled environment chambers ventilated with CFA where the fruit were maintained at 13 °C, 95% RH in the dark. Afterwards, fruit tissue was frozen in liquid nitrogen and stored at −80 °C prior to protein extraction. In wounded fruit, plant tissue was sampled from the opposite side of the wound (i.e. 'healthy tissue'), as our aim was to check the systemic response of fruit to ozone and not the direct response to wounding/pathogen. The fumigation system was described in previous studies (Tzortzakis et al., 2007).

2.2. Protein extraction

A phenol (Phe)-based extraction procedure was adapted from that described by Saravanan and Rose (2004). Five grams of frozen plant tissue were finely powdered in liquid nitrogen using a pestle and mortar prior to resuspension in 15 mL of extraction buffer [buffer 1: (1%, w/v polyvinylpolypyrrolidone (PVPP), 0.7 M sucrose, 0.1 M KCl, 0.5 M Tris–HCl pH 7.5, 500 mM EDTA, 1 mM phenylmethane-sulfonyl fluoride (PMSF) and 2%, v/v β-mercaptoethanol)]. The mixture was homogenised (Ultra Turrax T25, IKA Labortechnik, Staufen, Germany) on ice in a fume hood (at ~2–3 °C for 30 min in increments of less than 1 min to prevent sample warming) then an equal volume of Tris–HCl (pH 7.5)-saturated Phe was added and the mixture re-homogenised on

ice for a further 30 min (at ~2–3 °C) prior to centrifugation (Sorvall RC-5B Plus, Dupont, Wilminghton, USA) at 12,000 × *g* for 30 min at 4 °C. The upper Phe phase was removed and re-extracted two more times with extraction buffer 1 as above. Protein aliquots were precipitated from the final Phe phase using five volumes of saturated ammonium acetate in methanol. The operation was performed overnight at −20 °C prior to pelleting proteins via centrifugation at 4 °C at 12,000 × *g* for 30 min. The recovered pellets were washed with ice-cold methanol, followed by multiple washes (2–3 times) with ice-cold acetone, dried on ice in a flow of nitrogen and stored to −80 °C prior to protein analysis. Protein concentration was quantified using the method of Bradford (1976), employing BSA as standard at 595 nm. Protein determination was also checked by employing bicinchoninic acid (BCA) protein assay at 562 nm (Smith et al., 1985).

2.3. SDS-PAGE analysis

One-dimensional SDS-PAGE analysis was carried-out with pre-casted gels using DeStreak rehydration solution (Cat. No.17-6003-19; Amersham Biosciences, Uppsala, Sweden). Solubilised proteins (30 μg protein per lane) were separated on 12% SDS-PAGE gels (21 cm × 25 cm × 0.15 cm) with an Ettan Dalt six-gel apparatus (Amersham Biosciences, Uppsala, Sweden) at 100 V for approximately 15 h. The gels were stained with silver stain (as described below) and image analysis performed with a Fluor-S™ Multi-Imager (BioRad, Hercules, CA, USA). For calibration of molecular masses, protein marker (14–200 kDa; Invitrogen, Paisley, UK) was used. All one-dimensional SDS-PAGE gels were repeated 4 times per treatment.

2.4. 2D gel electrophoresis, first and second dimension separation of proteins

2.4.1. First dimension separation

Dried protein precipitate was solubilised in DeStreak rehydration solution (Amersham Biosciences, Uppsala, Sweden), and 55 μg of total protein was used for isoelectric focusing (IEF) in a 4–7 pH gradients. DeStreak rehydration solution (340 μL) containing 0.5% carrier ampholytes immobilised pH gradient (IPG) buffer (4–7) (Amersham Biosciences) and IPG cover fluid (Amersham Biosciences) were used for IEF. Immobilised pH gradient strips (180 mm × 3 mm 4–7, Amersham Biosciences) were allowed to rehydrate for 14 h at 20 °C in strip holders without voltage. Proteins were focused at 20 °C in an IPGphor electrophoresis unit (Amersham Biosciences), using a four-step procedure, following manufacture instructions (Amersham Biosciences). Isoelectric focusing was completed when an accumulated voltage of 35,300 Vh was reached.

2.4.2. Second dimension separation

After focusing, proteins were reduced by incubating (equilibrating) IPG strips in equilibration buffer [6 M urea, 30% (v/v) glycerol, 2% (w/v) SDS, and 1.5 M Tris–HCl, pH 8.8] including DTT (3.5 mg mL^{-1}) for 15 min and alkylated for 15 min at room temperature with (45 mg mL^{-1}) iodoacetamide in the same buffer following the addition of a few grains of bromophenol blue.

The strips were placed on the top of a 12% SDS-PAGE gel (21 cm × 25 cm × 0.15 cm) containing; 40% (v/v) of 30% (w/v) acrylamide/Bis solution (Bio-Rad Laboratories, Hercules, CA, USA); 25% (v/v) buffer [1.5 M Tris (pH 8.8), 10% (w/v) SDS]; 0.5% (v/v) of 10% (w/v) ammonium persulphate (APS); 0.09% (v/v) N,N,N′,N′-tetramethyethylenediamine (TEMED) and covered with a layer of agarose (0.5% agarose in SDS running-buffer) (25 mM Tris, pH 8.3, 192 mM Glycine, 0.1% SDS). Ettan Dalt six gel system (Amersham Biosciences) was employed for 2D electrophoresis, using 1× SDS running buffer for the bottom (anode side) and 2× for the top (cathode side) of the acrylamide gels. Electrophoresis was performed at 1.5 W per gel for *c.* 20 h until the bromophenol dye front had migrated to the bottom of the gel. For calibration of molecular masses, protein marker (14–200 kDa; Invitrogen, Paisley, UK) was used. Several extracts were made from tomato fruit and at least three electrophoretic separations were performed per treatment.

2.5. Silver staining

Trials employing Coomassie Brilliant Blue R-250 to stain gels resulted in poor protein definition (unpublished data), so all figures and analysis were restricted to silver-stained gels. Proteins were detected by silver staining using SilverQuest™ Silver Staining Kit (Cat. No: LC6070; Invitrogen, Paisley, UK). Gels were incubated overnight in a fixative solution (40% (v/v) ethanol; 10% (v/v) acetic acid made with ultrapure water; >18.2 mΩ Millipore water) with gentle rotation, then incubated with 30% (v/v) ethanol for 10 min. Gels were then incubated in sensitising solution (30% (v/v) ethanol; 10% (v/v) sensitiser) for 10 min, in 30% (v/v) ethanol for 10 min and washed with ultrapure water (>18.2 mΩ Millipore water) for 10 min. Gels were stained in 1% (v/v) stainer solution for 15 min prior to washing with ultrapure water for 25 s. Colouration was developed within 6–15 min of incubation in developer solution (10% (v/v) developer plus one drop of enhancer). Stain development was stopped by the addition of 10 mL of stopper solution plus 10 min incubation. Finally, gels were washed with ultrapure water for 10 min. Throughout the whole staining procedure gels were treated separately in 200 mL of each solution.

2.6. Image analysis

Once stained, 2D gels were scanned with a UV/visible transmission scanner (ProXPRESS 2D, PerkinElmer, Boston, USA). Prior to the final scan, all gel images (16-bit) were scanned at 100 μm resolution for 1 s to ensure that the image intensity was linear between 15,000 and 55,000 units. Gel image analysis was performed using Progenesis image analysis software (Nonlinear Dynamics, Durham, NC, USA) using a semiautomated procedure, with manual correction and editing of spot features created by automatic default spot analysis settings. For comparison of different gel images, the false-colour overlay function incorporated within this software was utilised. In the overlay mode the spots of the reference gel (control: average of three) were displayed in magenta (<−1.5-fold) while the spots in the second gel (treated: average of three) were displayed in green (>1.5-fold). Overlaid matching spots appear black due to the complementary pseudocolour display, with no matching spots remaining magenta or green. Gels were cropped to remove areas of no interest, averaged in groups, the background removed, spot detection synchronised and then normalised to the average gels.

2.7. Mass spectrometry (MS) analysis and protein sequence determination

Protein spots were excised from 2D gels using an Ettan spot picker (Amersham Bioscience). The gel plugs were washed and sequentially incubated with reducing and alkylating reagents and with modified trypsin (Promega, Madison, WI, USA). Peptides were eluted from $ZipTip_{C18}$ and re-extracted in 50 μL 50% (v/v) acetonitrile (ACN)/0.1% (v/v) trifluoroacetic acid (TFA), prior to evaporation in a Speedvac (ThermoSavant, Milford, MA, USA) to 5 μL or 10 μL and mixed with an equal volume of 10 mM alpha-cyano-4-hydroxycinnamic acid (CHCA), and spotted directly on a MALDI target plate. Peptide mass fingerprinting was conducted using a low-resolution linear MALDI-time-of-flight (MALDI-TOF) mass spectrometer (Voyager-DE™ STR, Applied Biosystems, Foster

city, CA, USA). Mass spectra were recorded in positive reflector mode at a maximum accelerating potential of 20 kV in both manual and automatic modes. Mass spectra were obtained by averaging 1000 laser shots. External calibration of the standard spectra was performed using trypsin autolysis products (calibration 'Mixture 2'; Applied Biosystems, Foster city, CA, USA). Spectra were analysed and peak-lists generated using Data Explorer 4.0 Spectrum Analysis software, prior to database searching with MASCOT software (Matrix Science, London, UK). Peptide mass data were analysed for corresponding protein matches in the National Centre of Biotechnology Information (NCBI), Swiss-Prot and the tomato gene index (http://compbio.dfci.harvard.edu/cgi-bin/tgi/gimain.pl?gudb=tomato) from The Institute for Genome Research (TIGR) primary sequence databases (compares peptide sequences and their theoretical fragmentation patterns with a given MS/MS protein profile) with 50 ppm mass accuracy and 0–2 peptide cleavage site-settings on the MASCOT search engine. The database ranks matched proteins according to the molecular weight search (MOWSE) score, the mass error margin and the sequence coverage by matched peptides. The MOWSE score is a molecular weight scoring algorithm which provides an indication of the certainty of identification; the higher the score, the more confidence in identification and additional experimental confirmation conducted in case of multiple matches employing *M*r and p*I* of the protein, based on 2DE studies with plants of the same family (including *N. tabacum* L. and *S. tuberosum* L.).

2.8. Statistical analysis

Silver-stained spots were quantified on the basis of their volume after gel normalisation and background subtraction, and significance differences determined using *t*-test or non-parametric Wilcoxon tests.

3. Results

3.1. Impact of ozone-enrichment and/or wound-inoculation with *B. cinerea* on protein yield

Quantitative comparison of protein yield employing Bradford and BCA assays was conducted in tomato fruit subjected to ozone and/or wound-inoculation with *B. cinerea* are summarised in Table 1. Atmospheric ozone-enrichment was shown to significantly ($P < 0.05$) increase protein yield (27–50%) in comparison with fruit maintained throughout in CFA, but the effect did not persist when fruit were removed from an ozone-enriched atmosphere. This effect was mainly due to an increase in large proteins (>45 kDa, Fig. 2). A similar pattern of change in protein content was observed in wound-inoculated fruit treated with ozone.

3.2. Impacts of atmospheric ozone-enrichment and/or wound-inoculation with *B. cinerea* on protein composition of tomato fruit visualised by one-dimensional SDS-PAGE

To see if ozone treatment and/or wound-inoculation with *B. cinerea* resulted in significant change in protein composition of the fruit, protein profiles were established using one-dimensional SDS-PAGE prior to two-dimensional gel electrophoresis and compared between treatments. Although the amount of proteins loaded on the gel varied slightly for the different treatments there were clearly identifiable differences in protein profiles (as shown in Fig. 2), suggesting significant changes in protein composition of the fruit tissue subjected to ozone and/or wound-inoculation with *B. cinerea*. Thus, atmospheric ozone-enrichment was shown to significantly ($P < 0.05$) increase protein yield in comparison with fruit maintained throughout in CFA, but the effect did not persist when fruit were removed from an ozone-enriched atmosphere. Further protein analyses were conducted using two-dimensional gels followed by protein identification using MALDI-TOF spectrometry.

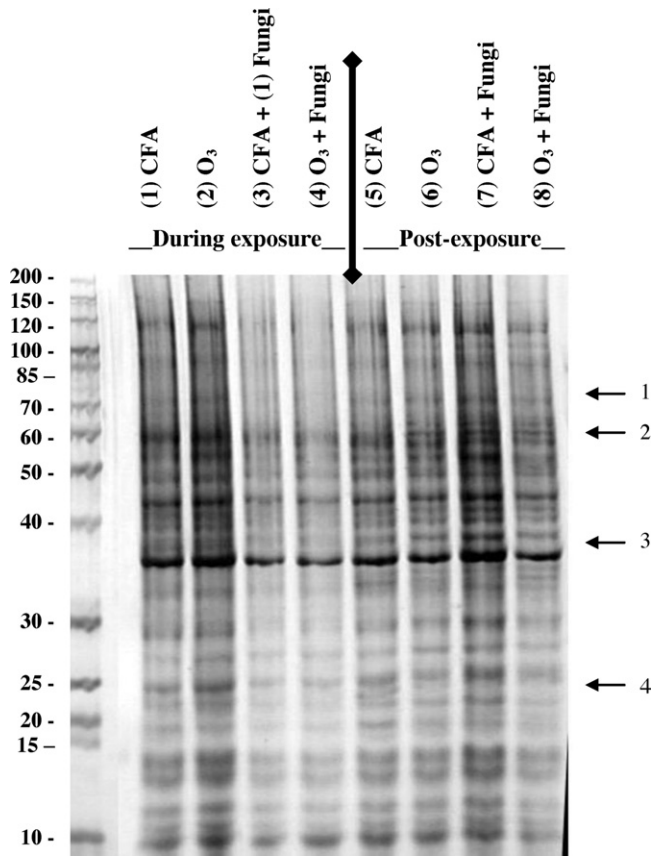

Fig. 2. Impacts of atmospheric ozone-enrichment (0.05 μmol mol^{-1}) and/or wound-inoculation with *B. cinerea* on protein content of tomato fruit. SDS-PAGE gels were silver stained. Labelled arrows indicate shifts in proteins.

3.3. Impacts of atmospheric ozone-enrichment and/or wound-inoculation with *B. cinerea* on protein composition of tomato fruit visualised by two-dimensional gel electrophoresis

The same samples subjected to one-dimensional SDS-PAGE (Fig. 2) were evaluated by two-dimensional gel electrophoresis. Two-dimensional gel electrophoresis allowed the resolution of up to 218 protein spots per gel (Table 2). Small and weak spots, plus those not consistent between gels, were disregarded (spot filtering).

Preliminary efforts to optimise the *p*I range for 2D gels indicated a narrow (4–7) linear range in *p*I resulted in the best resolution of protein species, allowing the analysis of more than 80% of the proteins visualised within the 3–10 *p*I range (data not shown). Gels revealed a broad distribution in protein composition in ozone-treated and/or wound-inoculated tomato fruit both in terms of size (10,000–110,000 Daltons) and *p*I values.

Atmospheric ozone-enrichment and/or wound-inoculation with *B. cinerea* resulted in marked shifts in the tomato proteome. As shown in Fig. 3 a strong shift in tomato proteome was transiently induced in fruit exposed to ozone for 1 week compared to equal fruit maintained in ozone-free air (Fig. 3A). Transfer of ozone-treated fruit to "charcoal-filtered" air for 1 week reversed the proteome shift induced by ozone (Fig. 3B). Similarly, fruit wound-inoculated with *B. cinerea* have shown a marked shift in the proteome (Fig. 4Aa) compared to the control (Fig. 3Aa). This shift lasted for at least 2 weeks post inoculation (Fig. 4Ba). Interestingly, ozone-treatment

Table 1
Impacts of atmospheric ozone-enrichment (0.05 μmol mol^{-1}) and/or wound-inoculation with *B. cinerea* on protein content of tomato fruit. Values represent means (±SE) of three-to-four independent measurements per treatment. Values in adjacent columns (i.e. for individual assays) bearing the same superscripts show no significant difference at the 5% level.

Treatment	Protein yield (μg g^{-1} f.wt)			
	Bradford assay		BCA assay	
	CFA	Ozone	CFA	Ozone
(A) Sustained ozone-enrichment[a]	140.8 ± 5^{b}	178.5 ± 4^{a}	97.8 ± 4^{b}	152.1 ± 2^{a}
(B) Sustained ozone-enrichment + fungi	150.1 ± 7^{b}	224.0 ± 4^{a}	112.5 ± 18^{b}	153.2 ± 39^{a}
(C) Ozone-induced 'memory' effect	203.7 ± 6^{a}	198.4 ± 3^{a}	143.7 ± 24^{a}	116.8 ± 12^{a}
(D) Ozone-induced 'memory' effect + fungi	206.1 ± 12^{a}	219.7 ± 10^{a}	138.4 ± 35^{a}	147.4 ± 24^{a}

[a] Capital letters are referring to experimental treatments mentioned in Fig. 1.

Table 2
Impacts of atmospheric ozone-enrichment (0.05 μmol mol^{-1}) and/or wound-inoculation with *B. cinerea* on proteins levels of tomato fruit evaluated on 2D gels. Values represent means (±SE) of three-to-four independent measurements per treatment. Values bearing the same subscript in individual columns are not significantly different at the 5% level. Values in parenthesis represent shifts (compared to CFA) of individual proteins by at least 1.5-fold.

Number of protein spots	Increased	Decreased	Novel	Total
(A) Sustained ozone-enrichment[a]	54 ± 19^{a} (37)	83 ± 1^{a} (11)	51 ± 19^{a} (–)	137 ± 19^{b} (48)
(B) Sustained ozone-enrichment + fungi	98 ± 10^{a} (0)	60 ± 11^{a} (32)	28 ± 1^{ab} (–)	158 ± 0^{b} (32)
(C) Ozone-induced 'memory' effect	63 ± 56^{a} (2)	155 ± 56^{a} (97)	1 ± 1^{b} (–)	218 ± 0^{a} (99)
(D) Ozone-induced 'memory' effect + fungi	98 ± 18^{a} (11)	69 ± 18^{a} (16)	0^{b} (–)	167 ± 1^{b} (27)

[a] Capital letters are referring to experimental treatments mentioned in Fig. 1.

suppressed the proteome shift induced by wound-inoculated *B. cinerea* (Fig. 4Ab). The effect of ozone on the suppression of the proteome shift caused by the wound-inoculated *B. cinerea* lasted for at least 1 week after transfer of ozone-treated fruit to charcoal-filtered air (Fig. 4 Ba).

In order to probe the impacts of atmospheric ozone-enrichment among the treatments (see Figs. 3 and 4) in greater detail, 41 protein spots were selected for peptide fingerprinting (Fig. 5). Fifteen of these proteins were identified, eight from tomato (*L. esculentum* L.), one by similarity to the corresponding protein from potato (*S.*

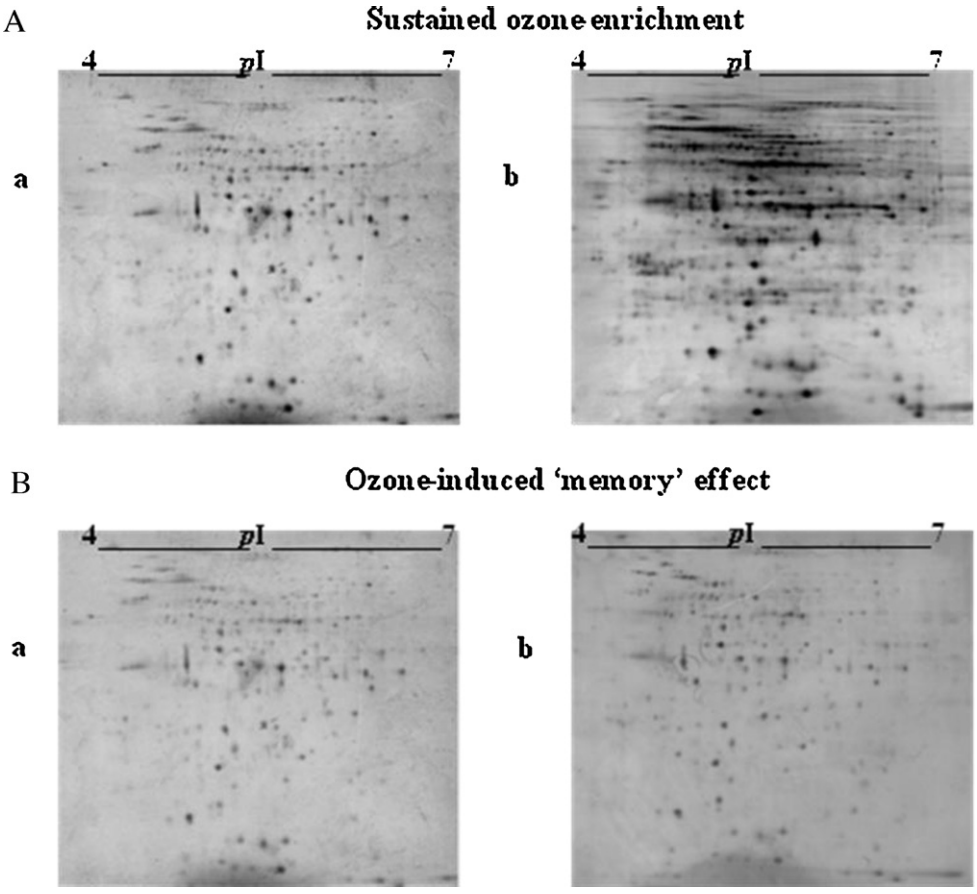

Fig. 3. Two-dimensional gels (*p*I 4–7) illustrating the protein composition of tomato fruit maintained in (a) charcoal-filtered 'clean air' (controls) or (b) sustained atmospheric ozone-enrichment at 0.05 μmol mol^{-1} (ozone-treated) for 1 week (A) or transferred/stored for 1 more week to 'clean air' following treatment to test for ozone-induced 'memory' effect (B).

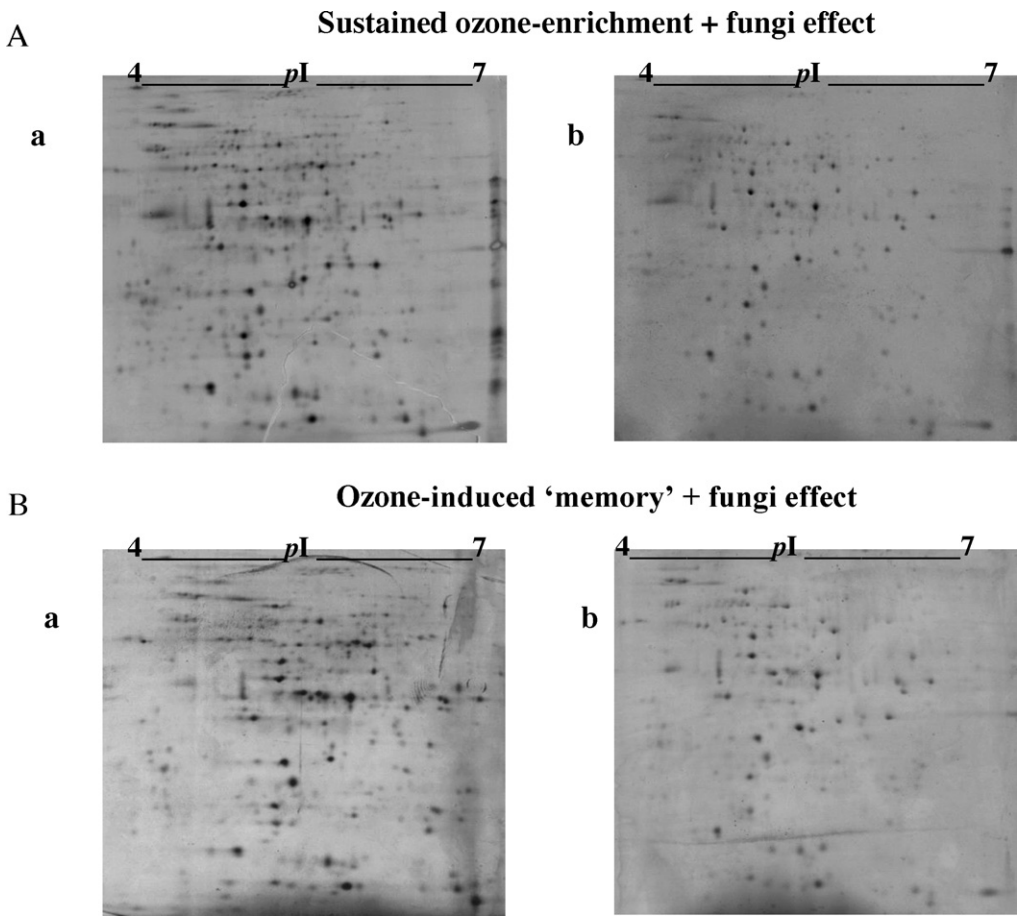

Fig. 4. Two-dimensional gels (*p*I 4–7) illustrating change in protein composition of tomato fruit after wound-inoculation with *B. cinerea* and maintained in (a) charcoal-filtered 'clean air' (controls) or (b) subjected to sustained atmospheric ozone-enrichment 0.05 μmol mol^{-1} (ozone-treated) for 1 week (A). Second batch of fruit were maintained in (a) charcoal-filtered 'clean air' (controls); (b) subject to sustained atmospheric ozone-enrichment 0.05 μmol mol^{-1} (ozone-treated) for 1 week then wound-inoculated with *B. cinerea* and transferred/stored for 1 week to 'clean air' following ozone-induced 'memory' effect (B).

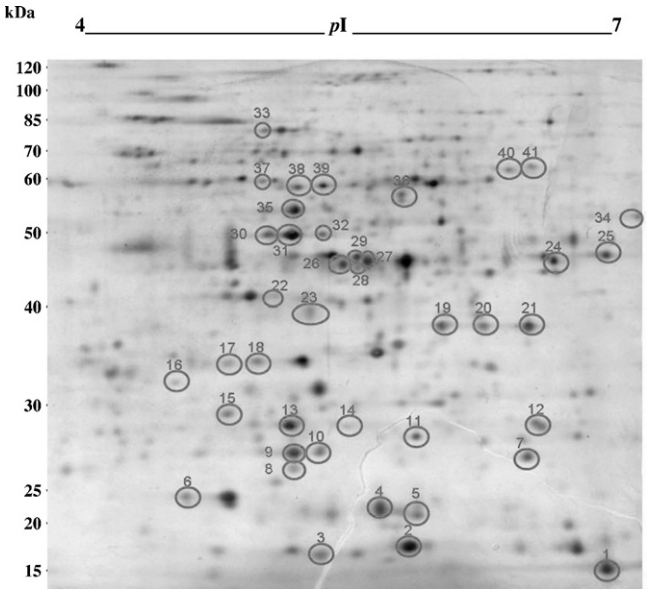

Fig. 5. Two-dimensional gels (*p*I 4–7) illustrating differential protein composition of tomato fruit maintained in charcoal-filtered 'clean air' (controls) or sustained atmospheric ozone-enrichment (0.05 μmol mol^{-1}) for 1 week then wound-inoculated with *B. cinerea* and transferred/stored for a week in 'clean air'. 2D-DIGE with controls labelled in magenta and ozone-treated labelled in green. Black spots indicate protein expression within 1.5-fold. Numbers refer to spots selected for detailed analysis.

tuberosum L.), two from rice (*O. sativa* L.), three from *A. thaliana* and one from *Pisum sativum* L (see Table 3). However there had to be some reliance on spot identification made by Saravanan and Rose (2004) and Casado-Vela et al. (2005) during their studies investigating responses to heat-stress or blossom-end rot in tomato fruit.

In order to identify the pattern of metabolic shifts induced by atmospheric ozone-enrichment and/or wounding/fungal attack, identified proteins have been grouped according to their functional association (Table 4). The first group comprises constitutive proteins such as chaperonin 21 (CPN21), malate dehydrogenase (MDH) and dehydrin (DHD). The second group comprises proteins allied to signalling and antioxidative metabolism including superoxide dismutase (SOD), thioredoxin peroxidase (TPX), IN2-1 glutathione transferase (IN2-1), ascorbate peroxidase (APX1) and 1-aminocyclopropane-1-carboxylate oxidase (ACO). A third group comprises enzymes associated with carbohydrate metabolism and the pentose phosphate pathway, including inorganic pyrophosphatase (PPase), invertase (INV) and glyceraldehyde 3-phosphate dehydrogenase (GAPDH). The fourth group comprises proteins associated with terpenoid and flavonoid biosynthesis including farnesyl pyrophosphate synthase (FPS) and dihydroflavonol-4-reductase (DFR). The fifth group comprises proteins that are associated with plant stress responses including protease-like protein (ULP) and 3-methylcrotonyl CoA carboxylase (3-MCC). Protein expression was differentially affected by respective treatments (see Table 5).

Table 3
Putative identification of proteins responsive to atmospheric ozone-enrichment (0.05 μmol mol^{-1}) and/or wound-inoculation with *B. cinerea*.

Spot no.	*p*I exp./ theor.	*M*r exp./ theor.	Database[a]	Score/ seq. cov./pept. match	Gene indices (gi) no/ accession no	Identification, putative function, species/EC[b]
1	6.76/ 5.70	13,398/ 22,228	S	2.09E + 04/ 45/6	gi:134,682/P14831	Superoxide dismutase (Cu–Zn), chloroplast precussor, *L. esculentum*/1.15.1.1
2	5.77/ 5.07	15,845/ 16,660	N	1.9E + 02/ 38/9	gi:2935459/AAC73051	Farnesyl pyrophosphate synthase, synthesis of farnesyl pyrophosphate, *L. esculentum*/2.5.1.1
3	5.37/ 5.36	15,321/ 9735	N	1.3E + 02/ 39/3	gi:19386765/BAB86146	Ulp1 protease-like, *O. sativa* (japonica cultivar-group)/
4	5.62/ 6.50	20,905/ 27,100	N	61/ 52/	gi:7446589/T06811	Dehydrin 2, *P. sativum*
5	5.82/ 6.10	21,305/ 19,860	N	4.65E + 03/ 41/17	gi:30841938/AAP34571*	Thioredoxin peroxidase, *L. esculentum*/1.11.1.-
11	5.82/ 6.80	29,202/ 26,562	N	6.59E + 05/ 55/12	gi:7331143/AAF60293*	Chaperonin 21 precursor, *L. esculentum*
13	5.24/ 6.80	30,701/ 26,562	N	6.59E + 05/ 55/12	gi:7331143/AAF60293*	Chaperonin 21 precursor, *L. esculentum*
14	5.50/ 6.10	30,650/ 22,467	N	3.9E + 03/ 24/4	gi:18201653/AAL65397	3-Methylcrotonyl CoA carboxylase biotin-containing subunit (fragment)-*O. sativa*/
15	4.96/ 5.20	31,589/ 29,969	T	2.81E + 10/ 64/14	gi:22655240/TC115830*	IN2-1 glutathione transferase, *A. thaliana*/2.5.1.18
17	4.96/ 5.81	34,610/ 33,056	T	2.22E + 04/ 34/9	gi:11358468/T49933*	Inorganic pyrophosphatase, *A. thaliana*/3.6.1.1
19	5.97/ 8.80	36,141/ 39,619	T	6.73E + 11/ 61/17	gi:21388544/CAD33240*	Putative NAD-dependent malate dehydrogenase, *S. tuberosum*/1.1.1.37
20	6.18/ 8.80	36,840/ 39,619	T	6.73E + 11/ 61/17	gi:21388544/CAD33240*	Putative NAD-dependent malate dehydrogenase, *S. tuberosum*/1.1.1.37
21	6.41/ 8.80	36,905/ 39,619	T	6.73E + 11/ 61/17	gi:21388544/CAD33240*	Putative NAD-dependent malate dehydrogenase, *S. tuberosum*/1.1.1.37
25	6.81/ 5.93	44,269/ 31,926	N	3.0E − 04/ 26/7	gi:2078298/AAB54003	Glyceraldehyde 3-phosphate dehydrogenase, *L. esculentum*/1.2.1.12
29	5.51/ 5.60	46,863/ 41,501	S	78/ 26/	gi:119640/P10967	1-Aminocyclopropane-1-carboxylate oxidase homolog (protein E8), *L. esculentum*/1.14.17.4
31	5.24/ 5.70	50,829/ 27,800	N	63/ 26/	gi:15223049/NP_172267	L-Ascorbate peroxidase 1 cytosolic, *A. thaliana*
32	5.39/ 6.20	50,274/ 42,717	N	6.1E + 02/ 19/5	gi:410490/CAA791549	Dihydroflavonol-4-reductase, *L. esculentum*/1.1.1.219
35	5.26/ 5.50	55,898/ 70,200	N	75/ 28/	gi:384332/ 1905419A#	Invertase, *L. esculentum*/3.2.1.26

Proteins labelled according to Casado-Vela et al. (2005) (*) and Saravanan and Rose (2004) (#). Protein analysis failed for spots 6–10, 12, 16, 18, 22–24, 26–27, 30, 33–34, 36–41.

[a] Database search corresponds to (S) Swiss-Prot, (N) NCBI and (T) TIGR.
[b] EC corresponds to the enzyme classification number.

Table 4
Identified protein grouped according to function.

Group	Identification/putative function	Abbreviations
(1) Constitutively expressed	Chaperonin 21	CPN21*
	NAD-dependent malate dehydrogenase	MDH*
	Dehydrin	DHD
(2) Signalling and antioxidative metabolism	Cu-Zn Superoxide dismutase	SOD
	Thioredoxin peroxidase	TPX*
	IN2-1 glutathione transferase	IN2-1*
	Ascorbate peroxidase	APX1
	1-Aminocyclopropane-1-carboxylate Oxidase	ACO
(3) Carbohydrate metabolism and pentose phosphate pathway	Glyceraldehyde 3-phosphate dehydrogenase	GAPDH
	Inorganic pyrophosphatase	PPase*
	Invertase	INV#
(4) Terpenoid and flavonoid biosynthesis	Farnesyl pyrophosphate synthase	FPS
	Dihydroflavonol-4-reductase	DFR
(5) Stress-associated function unknown	Protease like – protein	ULP
	3-methylcrotonyl CoA carboxylase	3-MCC

Proteins identified from 2DE run by Casado-Vela et al. (2005) (*) or Saravanan and Rose (2004) (#).

Table 5
Impacts of atmospheric ozone-enrichment (0.05 μmol mol^{-1}) and/or wound-inoculation with *B. cinerea* on levels of specific proteins in tomato fruit.

Spot no.	Protein	Sustained ozone-enrichment	Ozone-induced 'memory' effect	Sustained ozone-enrichment + fungi	Ozone-induced 'memory' effect + fungi
11,13	CPN21	—	↓	↓	↓
19,20,21	MDH	↑↓	↓	↓	—
4	DHD	↑	↓	↓	↓
1	SOD	—	—	—	↓
5	TPX	↑	↓	—	—
15	IN2-1	—	—	—	—
31	APX	—	↓	—	—
29	ACO	—	—	↓	↓
17	PPase	—	—	—	—
35	INV	—	↓	—	—
25	GAPDH	↓	↓	—	—
2	FPS	—	↓	—	—
32	DFR	↑	—	↓	—
3	ULP	↑	—	↓	—
14	3-MCC	↑	—	—	—

Protein expression (↓) down-regulated (<−1.5-fold); (↑) up-regulated (>1.5-fold) and (—) in unchanged behaviour within 1.5-fold. Numbering refers to spots selected for detailed analysis.

4. Discussion

The present study demonstrated that low-level ozone-enrichment results in marked changes in protein yield and composition in tomato fruit (see Tables 1 and 2). Wound/fungal-inoculation with *B. cinerea*, as a stress factor, resulted in a 7% increase in protein yield, and the down-regulation of 32 proteins. Ozone exposure markedly increased protein yield comparing with the equivalent control treatments, while ozone suppressed shifts in the proteome induced by wounding/fungal attack. However, the effect did not persist when fruit were removed from an ozone-enriched atmosphere.

This is possible due to protein alteration/function changes, but this needs further investigation.

Using a combination of 2DE, trypsin in-gel digestion, peptide mass fingerprinting, database search techniques and correspondence with the existing literature, 15 proteins of known function were tentatively identified. Most of the identified proteins were resolved as discrete spots on gels, but two proteins were resolved in two spots (chaperonin; CPN21) and another in three (malate dehydrogenase; MDH). Such multiplicity is consistent with the resolution of isoenzymes or post-translational modifications. Interestingly some proteins were expressed only in ozone-treated fruit (e.g. 3-MCC; spot 7 and 22) whereas others like SOD, which is involved in the detoxification of ROS, were expressed in fruit subjected to wounding/fungal attack.

The majority of the identified proteins exhibited shifts in protein expression in response to the treatments adopted in the present study, with only a few (such as IN2-1 and PPase) remaining unaffected. Inorganic pyrophosphatase involved in carbohydrate metabolism and IN2-1 are a group of related enzymes that hydrolyse sucrose to hexose sugars contributing to tomato fruit quality, both in terms of flavour and acids (Iwahashi and Hosoda, 2000). Constitutively-expressed proteins (group 1; see Table 4) tended to be increased by ozone-treatment, but protein abundance tended to decline following transfer to 'clean air' and/or wound-inoculation. These findings are generally consistent with the reported function of dehydrin in citrus as a scavenger of hydroxyl (Hara et al., 2005) and the perceived role of chaperonin in the optimal folding and protection of proteins under both normal and stress conditions (Ranford et al., 2000).

A number of the identified proteins are involved in the control of cellular oxidative status. Proteins related to oxidative metabolism (e.g. TPX) were induced during ozone exposure, but suppressed following transfer to 'clean air' (e.g. APX1). However, rather surprisingly, the same batch of oxy-responsive proteins did not appear sensitive to wound-inoculation with *B. cinerea*. Ascorbate peroxidase is involved in the detoxification of intracellular H_2O_2 and is induced in response to many environmental stresses including radiation, drought, wounding, mechanical damage, and extreme temperatures (Prasad et al., 1994; Yahraus et al., 1995). It is also believed to respond, at least at the level of gene expression, to pathogen attack (Mittler and Zilinskas, 1992). Thioredoxin peroxidase (a chloroplast-based protein) protects the photosynthetic machinery by reducing hydrogen peroxide (Prasad et al., 1994). Interestingly, and in accordance with the observed ozone-induced suppression of *Aco 1* gene expression (Tzortzakis et al., 2011), ACO protein abundance was markedly reduced in ozone-treated tomato fruit. In contrast, and again in accordance with the observed shifts in *Aco 1* gene expression induced by ozone in fruit subject to wounding/fungal attack (Tzortzakis et al., 2011), ACO protein abundance induced by wounding/fungal attack was suppressed by ozone-treatment, both during and following exposure to the gas. The ACO1 enzyme plays an important role in the production of ethylene and the observed down-regulation of this enzyme under ozone suggests that reduced ethylene production might be part of the mechanism of ozone-increased fruit resistance to pathogens. In contrast, IN2-1 did not appear responsive to ozone-treatment, consistent with reported unresponsiveness of this protein to herbicide treatments in maize (*Zea mays* L.) and soybean (*Glycine max* L. Merr.) (McGonigle et al., 2000), but at odds with the finding of Casado-Vela et al. (2005) who reported IN2-1b protein induction in tomato fruit in response to blossom-end-rot.

Protein expression involved in terpenoid or flavonoid biosynthesis varied among the treatments. Indeed, farnesyl pyrophosphate is a precursor of phytosterols, sesquiterpenoids, phytoalexins, and is involved in protein farnesylation, which plays an essential role in cell cycle progression (Chappell, 1995). Thus limitation in farnesyl pyrophosphate synthesis may affect the abundance of compounds essential in fruit growth and metabolism. Moreover, dehydroflavonol-4-reductase catalyses the last step in the flavonoid-biosynthesis pathway leading to anthocyanins and proanthocyanidins (Moyano et al., 1998).

Although there is a growing volume of literature dealing with the molecular genetics underlying bacterial- and fungal-plant pathogenesis (Hensel and Holden, 1996; Tzortzakis et al., 2011), few studies have addressed proteome modifications associated with such interactions (see Konishi et al., 2001; Rep et al., 2002). Recently, proteomic analysis has been widely used to explore the mechanism of resistance of various fruit induced by different exogenous factors in response to fungal pathogens, for example, peach induced by salicylic acid (SA) and yeast (Chan et al., 2007)

and sweet cherry induced by SA (Chan et al., 2008). Several studies report differential protein expression in susceptible host plants (Mehta and Rosato, 2001; Tahara et al., 2003), with one particular study of the plant pathogen *Xylella fastidiosa* revealing major changes in cellular and extracellular bacterial proteins, including toxins, adhesion-related proteins, antioxidant enzymes and proteases (Smolka et al., 2003).

In the present investigation, a 2DE approach was successfully employed to profile differential display patterns in proteins induced or post-translationally modified following exposure of tomato fruit to low level atmospheric ozone-enrichment ($0.05\ \mu mol\ mol^{-1}$) and/or wound-inoculation with *B. cinerea*. Our study highlights the importance of responses to oxidative stress in the protection of fresh produce against pathogens and suggests that down-regulation of ethylene signalling might slow pathogen growth on fresh produce.

Acknowledgements

This study was supported by finance provided by the National Research Foundation of Greece (IKY), The UK-Natural Environment Research Council, The Royal Society and The Commonwealth Scholarships Organization. We also thank Dr. J. Gray and Dr. N. Morris for assisting with proteins analysis and identification.

References

Barsan, C., Sanchez-Bel, P., Rombaldi, C., Egea, I., Rossignol, M., Kuntz, M., Zouine, M., Latché, A., Bouzayen, M., Pech, J.C., 2010. Characteristics of the tomato chromoplast revealed by proteomic analysis. J. Exp. Bot. 61, 2413–2431.

Bradford, M.M., 1976. A rapid and sensitive method for quantitation of microgram quantities of protein utilizing the principle of protein-dye-binding. Anal. Biochem. 72, 248–254.

Bykova, N.V., Hoehn, B., Rampitsch, C., Banks, T., Stebbing, J.A., Fan, T., Knox, R., 2011. Redox-sensitive proteome and antioxidant strategies in wheat seed dormancy control. Proteomics 11, 865–882.

Casado-Vela, J., Sellés, S., Martinez, R.B., 2005. Proteomic approach to blossom-end rot in tomato fruits (*Lycopersicon esculentum* Mill): antioxidant enzymes and the pentose phosphate pathway. Proteomics 5, 2488–2496.

Casado-Vela, J., Sellés, S., Martínez, R.B., 2006. Proteomic analysis of tobacco mosaic virus-infected tomato (*Lycopersicon esculentum* M.) fruits and detection of viral coat protein. Proteomics 6, 196–206.

Catalá, C., Howe, K.J., Hucko, S., Rose, J.K., Thannhauser, T.W., 2011. Towards characterization of the glycoproteome of tomato (*Solanum lycopersicum*) fruit using Concanavalin a lectin affinity chromatography and LC–MALDI-MS/MS analysis. Proteomics 11, 1530–1544.

Chan, Z., Qin, G., Xu, X., Li, B., Tian, S., 2007. Proteome approach to characterize proteins induced by antagonist yeast and salicylic acid in peach fruit. J. Proteome Res. 6, 1677–1688.

Chan, Z., Wang, Q., Xu, X., Meng, X., Qin, G., Li, B., Tian, S., 2008. Functions of defense-related proteins and dehydrogenases in resistance response induced by salicylic acid in sweet cherry fruits at different maturity stages. Proteomics 8, 4791–4807.

Chappell, J., 1995. Biochemistry and molecular biology of the isoprenoid biosynthetic pathway in plants. Annu. Rev. Plant Physiol. Plant Mol. Biol. 46, 521–547.

Chen, S., Gollop, N., Heuer, B., 2009. Proteomic analysis of salt-stressed tomato (*Solanum lycopersicum*) seedlings: effect of genotype and exogenous application of glycinebetaine. J. Exp. Bot. 60, 2005–2019.

Corpillo, D., Gardini, G., Vaira, A.M., Basso, S.A., Accotto, G.P., Fasano, M., 2004. Proteomics as a tool to improve investigation of substantial equivalence in genetically modified organisms: the case of a virus-resistant tomato. Proteomics 4, 193–200.

Dahal, D., Heintz, D., Van Dorsselaer, A., Braun, H.P., Wydra, K., 2009. Pathogenesis and stress related, as well as metabolic proteins are regulated in tomato stems infected with *Ralstonia solanacearum*. Plant Physiol. Biochem. 47, 838–846.

Finnie, C., Andersen, B., Shahpiri, A., Svensson, B., 2011. Proteomes of the barley aleurone layer. A model system for plant signalling and protein secretion. Proteomics 11, 1595–1605.

Gammulla, C.G., Pascovici, D., Atwell, B.J., Haynes, P.A., 2011. Differential proteomic response of rice (*Oryza sativa*) leaves exposed to high- and low-temperature stress. Proteomics 11, 2839–2850.

Graham, D.M., Pariza, M., Glaze, W.H., Newell, G.W., Erdman, J.W., Borzelleca, J.F., 1997. Use of ozone for food processing. Food Technol. 51, 72–75.

Hahn, A., Bublak, D., Schleiff, E., Scharf, K.D., 2011. Crosstalk between Hsp90 and Hsp70 chaperones and heat stress transcription factors in tomato. Plant Cell 23, 741–755.

Hara, M., Fujinaga, M., Kuboi, T., 2005. Metal binding by citrus dehydrin with histidine-rich domains. J. Exp. Bot. 56, 2695–2703.

Hensel, M., Holden, D.W., 1996. Molecular genetic approaches for the study of virulence in both pathogenic bacteria and fungi. Microbiology 142, 1049–1058.

Huang, C., Verrillo, F., Renzone, G., Arena, S., Rocco, M., Scaloni, A., Marra, M., 2011. Response to biotic and oxidative stress in *Arabidopsis thaliana*: analysis of variably phosphorylated proteins. J. Proteomics 74, 1934–1949.

Iwahashi, Y., Hosoda, H., 2000. Effect of heat stress on tomato fruit protein expression. Electrophoresis 21, 1766–1771.

Konishi, H., Ishiguro, K., Komatsu, S., 2001. A proteomics approach towards understanding blast fungus infection of rice grown under different levels of nitrogen fertilization. Proteomics 1, 1162–1171.

Liu, L., Bai, L., Luo, C., Huang, D., Chen, M., 2011. Systematic annotation and bioinformatics analyses of large-scale *Oryza sativa* proteome. Curr. Protein Pept. Sci. 12, 621–630.

McGonigle, B., Keeler, S., Lau, S.C., Koeppe, M., O'Keefe, D., 2000. A genomics approach to the comprehensive analysis of the glutathione *S*-transferase gene family in soybean and maize. Plant Physiol. 124, 1105–1120.

Mehta, A., Rosato, Y.B., 2001. Differentially expressed proteins in the interaction of *Xanthomonas axonopodis* pv. *citri* when leaf extract of the host plant. Proteomics 1, 1111–1118.

Minas, I.S., Karaoglanidis, G.S., Manganaris, G.A., Vasilakakis, M., 2010. Effect of ozone application during cold storage of kiwifruit on the development of stem-end rot caused by *Botrytis cinerea*. Postharvest Biol. Technol. 58, 203–210.

Mittler, R., Zilinskas, B.A., 1992. Molecular cloning and characterization of a gene encoding pea cytosolic ascorbate peroxidase. J. Biol. Chem. 267, 21802–21807.

Moyano, E., Portero-Robles, I., Medina-Escobar, N., Valpuesta, V., Muñoz-Blanco, J., Caballero, J.L., 1998. A fruit-specific putative dihydroflavonol 4-reductase gene is differentially expressed in strawberry during the ripening process. Plant Physiol. 117, 711–716.

Overmyer, K., Tuomine, H., Kettunen, R., Betz, C., Langebartels, C., Sanderman, H.J., Kangasjärvi, J., 2000. Ozone-sensitive *Arabidopsis* rcd1 mutant reveals opposite roles for ethylene and jasmonate signalling pathways in regulating superoxide-dependent cell death. Plant Cell 12, 1849–1862.

Prasad, T.K., Anderson, M.D., Martin, B.A., Stewart, C.R., 1994. Evidence for chilling-induced oxidative stress in maize seedlings and a regulatory role for hydrogen peroxide. Plant Cell 6, 65–74.

Rabilloud, T., 2000. Proteome Research: Two-dimensional Gel Electrophoresis and Identification Methods. Springer, Berlin, pp. 247.

Ranford, J.C., Coates, A.R.M., Henderson, B., 2000. Chaperonins are cell-signalling proteins: the unfolding biology of molecular chaperones. In: Expert Reviews in Molecular Medicine. Cambridge University Press (http://www-ermm.cbcu.cam.ac.uk/00002015h.htm).

Rao, M.V., Lee, H.I., Creelman, R.A., Mullet, J.E., Davis, K.R., 2000. Jasmonate perception desensitises O_3-induced salicylic acid biosynthesis and programmed cell death in *Arabidopsis*. Plant Cell 12, 1633–1646.

Rep, M., Dekker, H.L., Vossen, J.H., de Boer, A.D., Houterman, P.M., Speijer, D., Back, J.W., de Koster, C.G., Cornelissen, B.J.C., 2002. Mass spectrometric identification of isoforms of PR proteins in xylem sap of fungus-infected tomato. Plant Physiol. 130, 904–917.

Rice, R.G., 2002. Century 21-pregnant with ozone. Ozone Sci. Eng. 24, 1–15.

Saravanan, R.S., Rose, K.C., 2004. A critical evaluation of sample extraction techniques for enhanced proteomic analysis of recalcitrant plant tissues. Proteomics 4, 2522–2532.

Sarig, P., Zahavi, T., Zutkhi, Y., Yannai, S., Lisker, N., Ben-Arie, R., 1996. Ozone for control of postharvest decay of table grapes caused by *Rhizopus stolonifer*. Physiol. Mol. Plant Pathol. 48, 403–415.

Schilmiller, A.L., Miner, D.P., Larson, M., McDowell, E., Gang, D.R., Wilkerson, C., Last, R.L., 2010. Studies of a biochemical factory: tomato trichome deep expressed sequence tag sequencing and proteomics. Plant Physiol. 153, 1212–1223.

Smith, P.K., Krohn, R.I., Hermanson, G.T., Mallia, A.K., Gartner, F.H., Provenzano, M.D., Fujimoto, F.K., Goeke, N.M., Olsen, B.J., Klenk, D.C., 1985. Measurement of protein using bicinchoninic acid. Anal. Chem. 150, 76–85.

Smolka, M.B., Martins, D., Winck, F.V., Santoro, C.E., Castellari, R.R., Ferrari, F., Brum, I.J., Galembeck, E., Filho, H.D.C., Machado, M.A., Marangoni, S., Novello, J.C., 2003. Proteome analysis of the plant pathogen *Xylella fastidiosa* reveals major cellular and extracellular proteins and a peculiar codon bias distribution. Proteomics 3, 224–237.

Spotts, R.A., Peters, B.B., 1980. Chlorine and chlorine dioxide for control of d'Anjou pear decay. Plant Dis. 64, 1095–1097.

Tahara, S.T., Mehta, A., Rosato, Y.B., 2003. Proteins induced by *Xanthomonas axonopodis* pv. *passiflorae* with leaf extract of the host plant (*Passiflorae edulis*). Proteomics 3, 95–102.

Tonneijck, A.E.G., Leone, G., 1993. Changes in susceptibility of bean leaves (*Phaseolus vulgaris*) to *Sclerotinia sclerotiorum* and *Botrytis cinerea* by pre-inoculative ozone exposures. Neth. J. Plant Pathol. 99, 313–322.

Tzortzakis, N.G., Singleton, I., Barnes, J.D., 2007. Deployment of low-level ozone-enrichment for the preservation of fresh produce in cold storage. Postharvest Biol. Technol. 43, 261–270.

Tzortzakis, N.G., Taybi, T., Roberts, R., Singleton, I., Borland, A., Barnes, J.D., 2011. Low-level atmospheric ozone exposure induces protection against *Botrytis cinerea* with down regulation of ethylene-, jasmonate- and pathogenesis-related genes in tomato fruit. Postharvest Biol. Technol. 61, 152–159.

Xu, L., 1999. Use of ozone to improve the safety of fresh fruits and vegetables. Food Technol. 53, 58–62.

Yahraus, T., Chandra, S., Legendre, L., Low, P.S., 1995. Evidence for a mechanically induced oxidative burst. Plant Physiol. 109, 1259–1266.